A Bidirectional Buck/Buck Hybrid Converter Achieving 96.3% Charging and 91.4% Discharging Peak Efficiency for Alkaline-to-Li-Ion Replacement

Xuan Wu[1*], Caiyu Tong[1,2*], Yan Lu[3], Mo Huang[2], Yuan Gao[1]
Southern University of Science and Technology, Shenzhen, China[1]
University of Macau, Macau, China[2], Tsinghua University, Beijing, China[3]
*Equally Credited Authors, Email: gaoy@sustech.edu.cn, yanlu@tsinghua.edu.cn

***Abstract*—This paper proposes a bidirectional Buck/Buck hybrid converter for lithium-ion (Li-ion) battery applications as alkaline battery replacement. By applying modified always-dual-path topology with reverse buck mode, the converter features shared power-stage architecture supporting both forward (discharge) and reverse (charge) operation modes. Compared with conventional Li-ion to alkaline battery power management ICs, the proposed design significantly improves charging efficiency while reducing thermal dissipation. In discharge mode, due to the constant presence of the capacitor path, the inductor current remains below the output current, minimizing DCR conduction losses. The proposed converter delivers up to 2A output current at 1.5V in discharge mode and achieves 91.4% peak efficiency at 0.5A load current. In charge mode, it supports up to 1.5A current with 96.3% peak efficiency.**

***Keywords*—bidirectional Buck/Buck converter, lithium-ion batteries, shared power-stage, inductor current reduction**

I. Introduction

Rising environmental concerns over disposable alkaline batteries have highlighted the urgent need for sustainable energy solutions in portable electronic devices. Conventional alkaline batteries, which often contain toxic heavy metals, pose significant ecological risks due to improper disposal and chemical leakage, and they can also damage electronic products. In contrast, lithium-ion (Li-ion) batteries offer a more environmentally friendly alternative with their superior energy density, recyclability, and extended cycle life. However, directly implementing Li-ion batteries in traditional 1.5V systems (e.g., remote controls, toys, computer mice) is challenging due to voltage incompatibility and inefficient charging architectures. As illustrated in Fig. 1, existing solutions adopt a separated scheme that employs a linear regulator for charging Li-ion battery from a 5V source and a Buck converter delivering a 1.5V output for the loads from the battery. Linear chargers offer benefits such as ripple-free operation, compact size, and high precision [1]. However, their inherent power dissipation ($P_{loss} = (V_{IN} - V_{OUT}) \times I_{LOAD}$) limits efficiency, thereby negatively impacting device thermal management and overall system reliability.

As shown in Fig. 1, reusing the power stages of the charging and discharging circuits can provide higher efficiency and power density. However, conventional or hybrid Buck converters do not support reverse battery charging [2]. Although some hybrid Buck-Boost topologies can be modified to achieve the function of bidirectional Buck/Buck conversion [3], its conversion ratio does not match the requirements for converting 5V to the battery voltage and the battery voltage to 1.5V. For the conventional four-switch

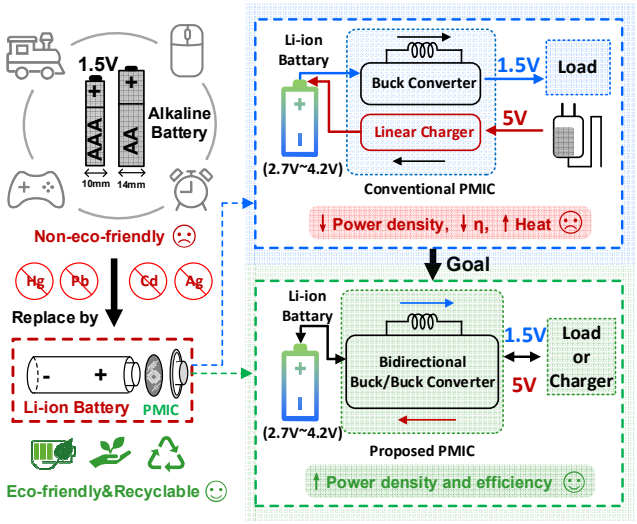

Fig. 1. Replacement of alkaline batteries with 1.5V AA/AAA Li-ion batteries.

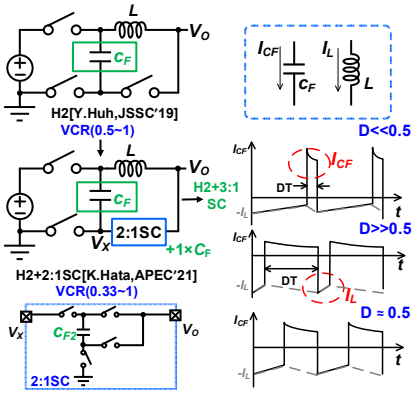

Fig. 2. Principle of dual-path converters.

Buck-Boost converter, the range of the voltage conversion ratio (VCR) can be satisfied, but the DCR loss of the inductor is relatively large.

Size is another critical consideration for this application. Dual-path hybrid converters can effectively reduce inductor current, thereby enhancing power density [4] [5]. However, as shown in Fig. 2, their VCR range is often limited. In critical VCR regions, an imbalance in the duty cycle (D) may occur. An excessively low D leads to excessive capacitor hard-charging current and increased losses. Conversely, a high D fails to effectively reduce the inductor current, resulting in higher DCR-related losses. Thus, designing a hybrid topology that effective reduces inductor current while maintaining an

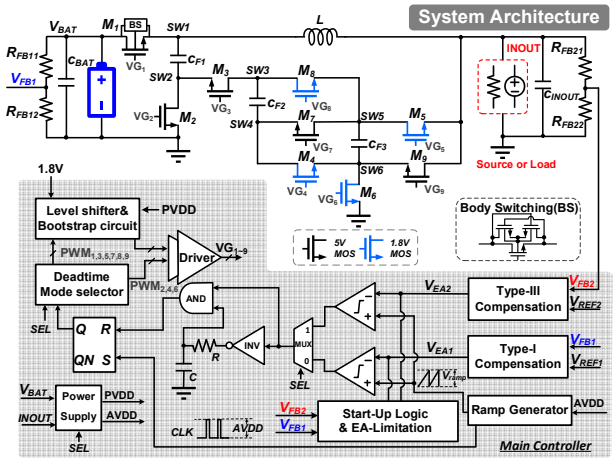

Fig. 3. Proposed bidirectional Buck/Buck hybrid converter.

optimal duty cycle for bidirectional Buck/Buck conversion remains challenging.

II. Proposed Bidirectional Buck/Buck Hybrid Converter

To address these limitations, based on always-dual-path topology, this paper proposes a bidirectional Buck/Buck hybrid converter optimized for the discharge voltage conversion ratio of lithium batteries and support efficient reverse charge mode. Building upon the structure in [2], a 3:1 switched-capacitor configuration is integrated to further extend the VCR range. Moreover, compared to prior works such as [4] and [5], which fail to simultaneously meet the VCR requirements for both charging ($0.54 < VCR < 0.84$) and discharging ($0.357 < VCR < 0.555$), the proposed topology not only extends the VCR range but also delivers high-efficiency power conversion across varying voltage conversion ratios through an optimized duty cycle range.

A. System Architecture

Fig. 3 presents the system architecture of the proposed bidirectional Buck/Buck hybrid converter. The power stage consists of five 5-V NMOS (M_1, M_2, M_3, M_7, M_9), four 1.8-V NMOS (M_4, M_5, M_6, M_8), three flying capacitors (C_{F1}, C_{F2}, C_{F3}), and two input/output capacitors.

The SEL signal functions as the charge/discharge mode selection signal. When SEL=1, the circuit operates in forward discharge mode, where the li-ion battery supplies power to the load. When SEL=0, the system enters reverse charge mode. AVDD and PVDD provide power to the control-stage circuits and gate drivers, respectively. During charging, the 5 V voltage from the INOUT terminal supplies power, while the li-ion battery provides power during discharging.

The controller has to deal with both modes. The discharge loop employs voltage-mode pulse-width modulation with Type-III compensation, while the charge loop utilizes a Type-I compensator as charge mode typically experiences no load transients. To ensure stable operation under various conditions, the error output signals V_{EA1} and V_{EA2} from both loops are clamped, and the duty cycle is limited to a range of 10% to 90%. During startup, the system implements fixed-duty-cycle switching to mitigate excessive instantaneous charging currents in the flying capacitors, preventing potential damage to the power switches.

B. Operation Principle and Timing Diagram

The operational principle of the proposed bidirectional Buck/Buck hybrid converter is illustrated in Fig. 4. When supplying power from the Li-ion battery to a 1.5V load (discharge mode), the converter configures the inductor to connect with the output terminal INOUT. In both switching states, the inductor current path (L-path) operates in parallel with the flying capacitor path (C_F-path), collectively delivering charge to the output. Since the flying capacitors provide additional current $\Delta Q_c/T$, the inductor current (I_L) can be reduced to $I_{Load}/$ (4-3D). This characteristic enables the use of smaller-form-factor inductors while maintaining equivalent conduction losses.

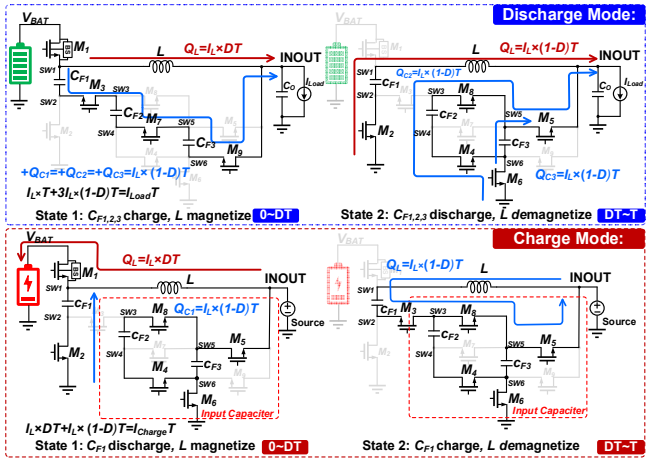

Fig. 4. Operation principle of the proposed converter.

During State 1, switches M_1, M_3, M_7, and M_9 are turned on, allowing the Li-ion battery to charge flying capacitors C_{F1}, C_{F2}, and C_{F3}. The node voltage V_{SW1} equals V_{BAT}, and the inductor current ramps up with a slope of $(V_{BAT}-V_{INOUT})/L$. In this state, both the inductor and the series-connected flying capacitors deliver power to the output. During State 2, switch M_2 turns on, forming a series connection between flying capacitor C_{F1} and the inductor, while C_{F2} and C_{F3} create a parallel path to simultaneously supply charge to the output. The node voltage V_{SW1} becomes $V_{BAT}-3V_{INOUT}$, with the current slope changing to $(V_{BAT}-4V_{INOUT})/L$. According to the volt–second balance of the inductor, the discharge conversion ratio is derived as $VCR = 1/(4-3D)$.

When converting a lithium battery voltage from 3.7 V to 1.5 V, the duty cycle is approximately 0.5, which effectively balances the losses between the flying capacitor and the inductor while avoiding extreme duty cycle conditions, thereby optimizing efficiency across different discharge stages of the lithium battery.

In reverse charge mode, switch M_9 remains off while switches M_4, M_5, M_6, and M_8 stay constantly on, with C_{F1} and C_{F2} serve as input capacitors. During State 1, M_1 and M_2 are turned on, enabling the parallel combination of inductor and flying capacitors to charge the Li-ion battery. The node voltage V_{SW1} equals V_{BAT}, with a current slope of $(V_{INOUT}-V_{BAT})/L$. In State 2, M_3 is turned on, allowing the inductor current to charge C_{F1}. The node voltage V_{SW1} becomes $V_{BAT}+V_{INOUT}$, with the current slope changing to $-V_{BAT}/L$. The charge mode conversion ratio is D ($0 < D < 1$). Notably, switches M_4, M_5, M_6, and M_8 experience a voltage stress of only 1.5V in all mode transitions, permitting the use of four 1.8-V NMOS transistors with better performance in the design.

Special consideration has been given to transistor sizing based on current handling requirements. Switch M_1, which carries the primary input/output current, is implemented with a larger size compared to other 5-V NMOS transistors. Similarly, switches M_5 and M_6 are sized twice as large as M_4 and M_8 to ensure balanced conduction losses across all devices. This optimized sizing strategy effectively distributes thermal dissipation while maintaining conversion efficiency.

A body switching architecture is employed to dynamically adjust the substrate potential of M_1 due to the voltage polarity reversal between V_{BAT} and V_{SW1} in different operation modes: during discharge mode ($V_{BAT} > V_{SW1}$) and charge mode ($V_{BAT} < V_{SW1}$).

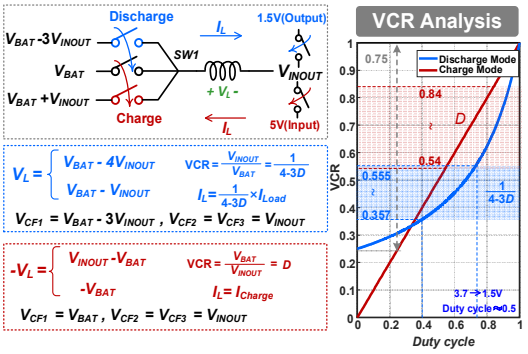

Fig. 5. Analysis of VCR in charge/discharge Modes.

C. Driver Impelementation

As shown in Fig. 6, the driving circuit for M_1 incorporates two bootstrap capacitors (C_{Boot1} and C_{Boot2}), implemented using on-chip MIM, MOM and MOS capacitors. When SEL=1 (discharge mode), transistor M_B remains off while M_A maintains conduction as C_{Boot2} charges, keeping the bottom plate of C_{Boot2} connected to node SW1. In this state, V_{BAT} charges C_{Boot1} through a Schottky diode (with associated forward voltage drop) when M1 is off, while C_{Boot1} and C_{Boot2} operate in parallel to power both the driver and level shifter when M_1 is on. Conversely, when SEL=0 (charge mode), M_A remains off and M_B stays on, connecting C_{Boot2}'s bottom plate to V_{BAT}. Similarly, V_{BAT} charges C_{Boot1} when M_1 is off, and the parallel-connected bootstrap capacitors supply the driving system when M_1 is on.

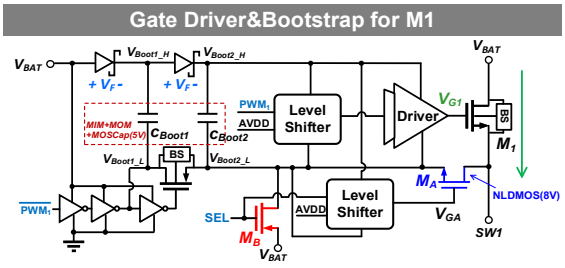

Fig. 6. Schematic of M_1 driver.

Fig.7 illustrates the driving circuit for transistors M_5 and M_8. To provide an enhanced V_{GS} voltage for the 8-V NLDMOS devices connected to the 1.8V power supply, an additional level shifter circuit is implemented. In this configuration, V_{Boot9H} represents the voltage at the upper plate of the bootstrap capacitor in M_9's driving circuit. During discharge mode, when M_9 is turned on, V_{Boot9H} reaches approximately the voltage across M_9's bootstrap capacitor plus the 1.5V output voltage. In this operational state, both M_5 and M_8 remain turned off, requiring the 1.8V supply to charge capacitor C_{Boot1}. When M_5 and M_8 need to be turned on, C_{Boot1} and C_{Boot2} operate in parallel to supply power to both the Driver and Level Shifter circuits. For charge mode operation, where flying capacitors C_{F1} and C_{F2} function as input capacitors while M_5 and M_8 maintain continuous conduction, C_{Boot1} serves to consistently replenish charge to C_{Boot2}.

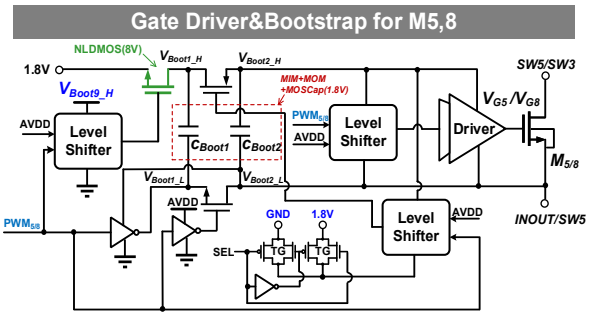

Fig. 7. Schematic of M_5/M_8 driver.

III. Measurement Results

The proposed hybrid converter was fabricated using a 180nm BCD process. Fig. 8 shows both the die and PCB micrographs. The three flying capacitors (10μF, 0402 package), the INOUT capacitor (22μF, 0402 package), and the battery capacitor (22μF, 0603 package) are arranged around the chip. Meanwhile, a 2.2-μH inductor (50-mΩ DCR, 4×4×1.65mm^3) is placed on the reverse side of the PCB. The battery voltage V_{BAT} ranges from 2.7 V to 4.2 V, and the output voltage is regulated to 1.5 V with a maximum load current of 2 A. The converter operates at a switching frequency of 2-MHz.

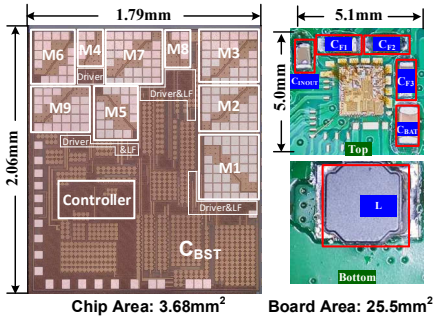

Fig. 8. Die micrograph and PCB.

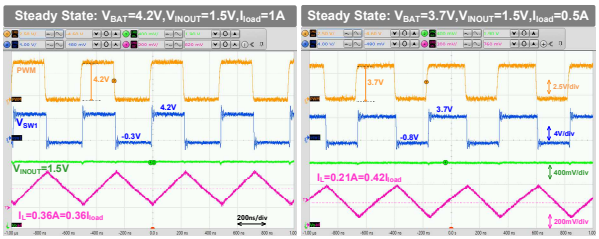

Fig. 9. Measured steady-state waveforms in discharge mode.

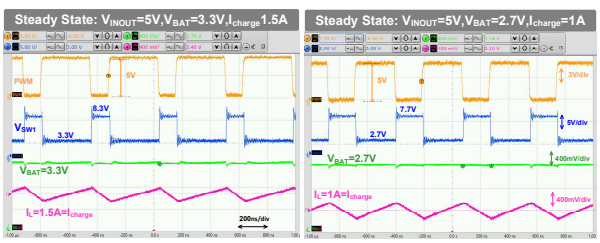

Fig. 10. Measured steady-state waveforms in charge mode.

Fig. 9 and Fig. 10 show the measured steady-state waveforms in discharge and charge modes, respectively. In discharge mode, V_{SW1} properly toggles between V_{BAT} and V_{BAT}-3V_{INOUT}, whereas in charge mode, it switches between V_{BAT} and V_{BAT}+V_{INOUT}. Both figures clearly show stable regulation and proper switching behavior, thereby validating the converter's bidirectional functionality. Fig. 11 presents the measured load transient in discharge mode. Overshoot (undershoot) is 87mV (98mV) for 1.2A to 0.2A (0.2A to 1.2A) load transient.

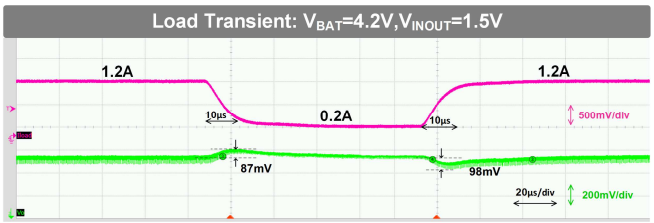

Fig. 11. Measured load transient in discharge mode.

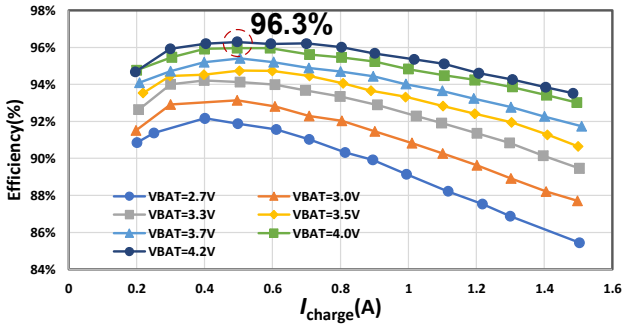

Fig. 12. Measured efficiency (Charge Mode).

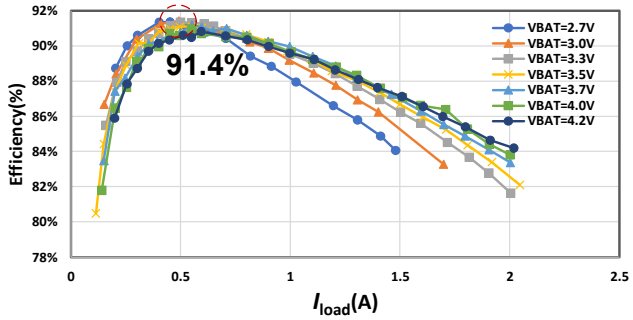

Fig.13. Measured efficiency (Discharge Mode).

Fig. 12 and Fig. 13 show the measured power conversion efficiencies in both modes. In charge mode, the converter achieves a peak efficiency of 96.3% at 5V input, 4.2V output, and 500mA charging current, while also delivering a maximum power of 6.3W and a power density of 2.28 W/mm². In discharge mode, as shown in Fig. 13, it reaches a peak efficiency of 91.4% at V_{BAT} = 3V and I_{load} = 500mA. The converter maintains high efficiency over a wide operating range in both modes. Table I summarizes and compare the performance of the proposed bidirectional converter with the state-of-the-art designs.

IV. Conclusion

This paper proposes a bidirectional Buck/Buck hybrid converter using modified always-dual-path topology with reverse buck mode, specifically designed for lithium-ion battery charging and discharging applications. The proposed architecture incorporates a parallel capacitor discharge path with the power inductor, which effectively reduces the inductor current while delivering high efficiency and current density. The converter reaches a peak discharge-mode efficiency of 91.4%, and a peak charge-mode efficiency of 96.3%. Simultaneously, it can achieve a discharge efficiency of over 90% across the entire input voltage range. Notably, the prototype's compact core test board, measuring just 5.1mm × 5.0mm, is significantly smaller than the cross-sectional area of conventional AA/AAA batteries, enabling seamless integration with alkaline-to-Li-ion replacement systems.

TABLE-I Comparison with State-of-the-art designs.

Process	EM6200B	JSSC'25 [6]	JSSC'24 [7]	This Work	
Topology	Buck Converter with 5V Linear Charger	Dual-C_F BoB	XC-SC Hybrid	Bidirectional Buck/Buck Hybrid	
Conversion Direction	Bidirectional	Unidirectional	Unidirectional	Bidirectional	
Conversion Type	Discharge :Buck, Charge: LDO	Buck-Boost	Buck	Discharge Mode: Buck	Charge Mode: Buck
V_{IN} [V]	2.7 ~ 4.2	2.7 ~ 4.2	2.7 ~ 4.2	2.7~4.2	5
V_{OUT} [V]	1.5/3	Sub1-6V	1 ~ 1.8	1.5	2.7~4.2
F_{SW} [MHz]	2.7	2	0.5	2	2
Max. I_{OUT} [A]	3.5	1	4.2	2	1.5
Max. P_{OUT} [W]	6	6	7.56	3	6.3
VCR Range	0~1	0.21-2.22	0.25 ~ 1	0.25~1	0~1
Max. I_{LDC} Reduction	I_{OUT}	I_{OUT}	0.125I_{OUT}	0.357I_{OUT}	I_{OUT}
Inductor [H]	N/A	1L: 1.2µ	2L: 4.7µ	1L:2.2µ	
Discrete Capacitor [F]	C_{OUT}: 10µ	$2C_{FLY}$: 4.7µ C_{OUT}: 1µ	$2C_{FLY}$: 22µ C_{OUT}: 4.7µ	$3C_{FLY}$: 10µ C_{INOUT}: 22µ,C_{BAT}: 22µ	
Chip Area [mm²]	N/A	4.16mm²	4.42mm²	3.68mm²	
**I_{OUT} Density [mA/mm²]	N/A	240	950	543	407
**P_{OUT} Density [W/mm²]	N/A	1.44	1.71	0.815	2.28
Peak Efficiency	*89%（Vo=1.5V）	*89%(Vo=2V)	91%	91.40%	96.30%
@VCR (I_{OUT})	@0.405(600mA)	@0.47(200mA)	@0.54(600mA)	@0.5(500mA)	@0.84(500mA)

*Estimated from the reported data, **Normalized to chip area

Acknowledgment

This work was supported in part by the National Natural Science Foundation of China under Grant No. 62004090, the Shenzhen Science and Technology Innovation Commission under Grant No. JCYJ20220818100216035, KJZD20240903 104021027, and JSGG20220831093401003.

References

[1] T.-C. Huang, R.-H. Peng, T.-W. Tsai, K.-H. Chen, and C.-L. Wey, "Fast charging and high efficiency switching-based charger with continuous built-in resistance detection and automatic energy deliver control for portable electronics," *IEEE J. Solid-State Circuits*, vol. 49, no. 7, pp. 1580-1594, Jul. 2014.

[2] J.-Y. Ko, Y. Huh, M.-W. Ko, G.-G. Kang, G.-H. Cho, and H.-S. Kim, "A 4.5V-input 0.3-to-1.7V-output step-down always-dual-path DC-DC converter achieving 91.5%-efficiency with 250mΩ-DCR inductor for low-voltage SoCs," in *Prof. Symp. VLSI Circuits*, Jun. 2021, pp. 1-2.

[3] Z. Tong, J. Huang, Y. Lu, and R. P. Martins, "A 42W reconfigurable bidirectional power delivery voltage-regulating cable," in 2023 *IEEE Int. Solid-State Circuits Conf.* (*ISSCC*), *Dig. Tech.Papers*, Feb. 2023, pp. 192-194.

[4] Y. Huh, S.-W. Hong, and G.-H. Cho, "A hybrid structure dual-path step-down converter with 96.2% peak efficiency using 250-mΩ large-DCR inductor," *IEEE J. Solid-State Circuits*, vol. 54, no. 4, pp. 959-967, Apr. 2019.

[5] K. Hata, Y. Jiang, M.-K. Law, and M. Takamiya, "Always-dual-path hybrid DC-DC converter achieving high efficiency at around 2:1 step-down ratio," in 2021 *IEEE Applied Power Electronics Conference and Exposition (APEC)*, Phoenix, AZ, USA: IEEE, Jun. 2021, pp. 1302-1307.

[6] J. Ruan et al., "A hybrid buck-or-boost converter for fast-transient and wide-voltage-range applications with continuous output delivery current," *IEEE J. Solid-State Circuits*, pp. 1-13, 2025.

[7] Q. Ma et al., "A cross-coupled hybrid switched-capacitor buck converter with extended conversion range and enhanced DCR loss reduction," *IEEE J. Solid-State Circuits*, vol. 59, no. 10, pp. 3192-3203, Oct. 2024